RSC Advances



REVIEW

View Article Online
View Journal | View Issue



Cite this: RSC Adv., 2022, 12, 32569

Self-healable fiber-reinforced vitrimer composites: overview and future prospects

Harsh Sharma,†^a Sravendra Rana, (1) †*^a Poonam Singh,^a Mikihiro Hayashi, (1) *^b Wolfgang H. Binder, (1) *^c Elisabeth Rossegger, (1) Ajay Kumar (1) and Sandra Schlögl (1) *^c

To achieve sustainable development goals, approaches towards the preparation of recyclable and healable polymeric materials is highly attractive. Self-healing polymers and thermosets based on bond-exchangeable dynamic covalent bonds, so called "vitrimers" could be a great effort in this direction. In order to match the industrial importance, enhancement of mechanical strength without sacrificing the bond exchange capability is a challenging issue, however, such concerns can be overcome through the developments of fiber-reinforced vitrimer composites. This article covers the outstanding features of fiber-reinforced vitrimer composites, including their reprocessing, recycling and self-healing properties, together with practical applications and future perspectives of this unique class of materials.

Received 15th August 2022 Accepted 2nd November 2022

DOI: 10.1039/d2ra05103f

rsc.li/rsc-advances

^eUniversity of Petroleum & Energy Studies (UPES), School of Engineering, Energy Acres, Bidholi, Dehradun, 248007, India. E-mail: srana@ddn.upes.ac.in

Chair of Macromolecular Chemistry, Institute of Chemistry, Faculty of Natural Science II, Martin Luther University Halle-Wittenberg, Von-Danckelmann-Platz 4, Halle, 06120, Germany. E-mail: wolfgang.binder@chemie.uni-halle.de

^aChemistry of Functional Polymers, Polymer Competence Center Leoben GmbH, Roseggerstraße 12, A-8700 Leoben, Austria. E-mail: sandra.schloegl@pccl.at

† Authors made equal contribution.

1. Introduction

Owing to their extraordinary properties including lightweight, strength, and stiffness, fiber-reinforced polymer composites are highly in demand for a wide range of applications including transportation, wind power, aerospace, and many others.¹⁻³ However, the wide use of thermoset materials represents a major challenge for closed material cycles as, after regular use, they are either converted into thermal energy, put into landfill, or their true recycling requires a significant amount of energy, thus driving researchers to search for alternative material concepts that display enhanced lifetimes *via* self-healing or recycling/reprocessing.^{4,5} The principal weakness of polymer composites is their damage by impact or chemical degradation, where the



Harsh Sharma was born in Gwalior, India, in 1995. He received B.E. degree in mechanical engineering from the RGPV, Bhopal, India, in 2016, and the M. Tech. degree in machine design from LPU, Punjab, India (2018). From 2018 to 2020, he has worked as Assistant Professor at DBUU, Dehradun, India. He is currently pursuing his PhD degree with the University of Petroleum and Energy

Studies (UPES), Dehradun, India. His research interests include nanotechnology, self-healing materials, advanced composites, and materials for sustainability.



Sravendra Rana is currently a Associate Professor in Applied Science Cluster (School of Engineering; UPES). Prior to joining UPES as Assistant Professor in June 2016, he worked as a postdoc at Martin Luther University Halle-Wittenberg, Germany (2012–2016; Prof. Wolfgang H. Binder Group), and Nanyang Technological University (NTU), Singapore (2011–2012). He received his PhD from Konkuk

University Seoul, South Korea (2011). His research expertise is in the development of functional materials, heterogeneous catalysis, click chemistry, and self-healing materials.

^bDepartment of Life Science and Applied Chemistry, Graduated School of Engineering, Nagoya Institute of Technology, Showa-ku, Nagoya 466-8555, Japan. E-mail: hayashi. mikihiro@nitech.ac.jp

RSC Advances Review

resulting micro-cracks can propagate to allow delamination and breakage of the composites, resulting in the total loss of physical properties of the composites, in turn reducing the durability of materials, and generating wastes.^{6,7} Patch repair, resin injection, and scarf repair are the commonly used methods for repairing carbon fiber reinforced polymers (CFRP), although, these approaches disturb the geometry and weight as well as require highly skilled work force. Besides, these techniques are unable to detect and fill the cracks deep within the structures. The era of self-healing materials is gradually settling where scratches on the designed materials can seal up with a complete restoration.8-11 The whole idea of self-healing materials was inspired by nature where natural healing of wounds and cuts occur in the living species.12-14 Different concepts to generate materials that can repair autonomically or via external stimuli such as heat,16 light,17 or pressure, have been designed using various approaches such as microencapsulation technique and supramolecular chemistry.¹⁸ In the microencapsulation technique, microcapsules containing chemical reagents for healing were implemented in the resins. When the macroscopic cracks reach the microcapsules, the healing reagents are excluded from the microcapsules, which instantly triggers the healing of cracks. However, this healing can be operated only one time at the same location, with the preparation, cost and stability of microcapsules representing another obstacle.19-21 Alternative systems with supramolecular chemistry, non-covalent bonds like hydrogen bonds, $^{22-24}$ π - π stacking, 25,26 and metal-ligand bonds²⁷ have therefore been introduced in polymeric matrices to allow repeated and autonomic healing and thus elongation of a material's lifetime. Owing to the reversible nature of these supramolecular association, recyclable and self-healing resins can be achieved. A drawback therein is that the non-covalent



Mikihiro Hayashi received his degree from Nagoya University (Prof. Yushu Matsushita group) in 2015. During his doctor course, he had been selected as a JSPS research fellow (DC2) and experienced researches in ESPCI Paris-Tech (Prof. Ludwik Leibler) and in Shanghai Jiao Tong University (Prof. Xinyuan Zhu). He then rejoined Ludwik Leibler's group as a postdoc, and experienced

another postdoc in Prof. Masatoshi Tokita in Tokyo institute of technology. In 2017, he became an assistant professor in Prof. Akinori Takasu group (Nagoya institute of technology), and currently manages his own laboratory as a PI. His research interest is the design of functional cross-linked materials.



Elisabeth Rossegger obtained her Master degree in Technical Chemistry from Graz University of Technology in 2017 and finished her PhD in Polymer Engineering at Montanuniversitaet Leoben in 2021. She currently heads the research group 'Chemistry of Stimuli-Responsive and Bio-based Polymers' at the Polymer Competence Center Leoben (Austria) and is a lecturer at the Technical

University of Graz, teaching polymer photochemistry at M.Sc. level. Her research focuses on the synthesis of stimuli-responsive polymers, the preparation of bio-based and recyclable polymers, the development of covalent adaptable networks and additive manufacturing.



Wolfgang Binder is currently a Full Professor of Macromolecular Chemistry at the Martin University Halle-Luther Wittenberg. Born (1969) and raised in Vienna (Austria), he studied chemistry at University of Vienna and conducted a PhD in organic chemistry (1995). After postdoctoral stays (1995-1997) with Prof. (Emory University, Atlanta, USA) and Prof. Mulzer

(University of Vienna), he completed his habilitation at the TU Vienna (2004), where he was Associate Professor from 2004 to 2007. Subsequently, he moved to Halle as a Full Professor in 2007. His research interests include "click-chemistry", polymer synthesis, supramolecular chemistry, self-healing polymers, nanotechnology.



Sandra Schlögl currently heads the division 'Chemistry of Functional Polymers' at the Polymer Competence Center Leoben (Austria) and is a lecturer at Montanuniversitaet Leoben teaching courses at M.Sc. level in polymer photochemistry and in stimuli-responsive polymers. In 2008, she obtained her PhD in Technical Chemistry from Graz University of Technology and in 2017, she finished her habilita-

tion (post-doctoral lecturing qualification) in Macromolecular Chemistry. Her research centers on the synthesis of polymers with switchable properties, the preparation of covalent adaptable polymer networks and advancing crosslinking and surface modification routes for elastomers and thermosets.

Review RSC Advances

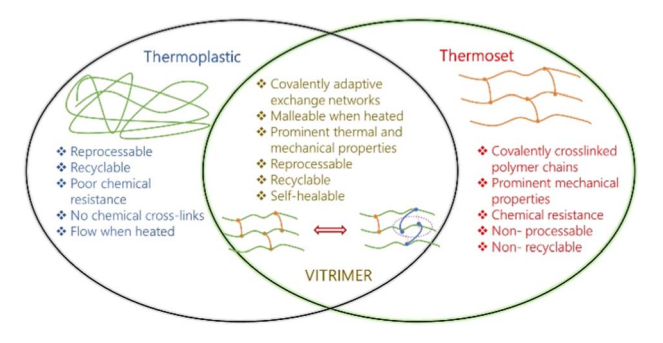


Fig. 1 Schematic representation of vitrimers' properties/advantages, compared with thermoplastic and thermoset.

bonding interactions can impart reduced mechanical properties and increased creep.²⁸

Based on the above background, a new generation of selfhealing polymers and thermosets operated with bondexchangeable dynamic covalent bonds, so-called "vitrimers", were reported by Leibler and co-workers.29 Vitrimers are a special type of network materials with dynamic covalent bonds, where the dynamic bond exchange occurs through the associative pathway. Unlike dissociative dynamic covalent bond (e.g. Diels-alder reaction or alkoxyamine radical exchange), the bond-exchange in associative dynamic covalent bond occurs without distinct separated steps of bond dissociation and re-association. Therefore on macroscopic timescales the network connectivity is never lost during the bond exchange in vitrimers, an outstanding feature that realizes unique functions.30,31 The development of vitrimers has extended the conventional classification of polymer materials (usually either thermoplastic or thermoset), where vitrimers exhibit thermoset polymer like mechanical properties/durability and also thermoplastic like malleability/processability at the same time (Fig. 1).32 In other words, vitrimers have combined advantages of both thermoset and thermoplastics polymers. Given the huge amount of unrecyclable waste from thermoset polymerbased products, the potential of the vitrimer concept is highly attractive, which meets the recently increasing demand to create polymers with efficient recyclability, together with the need to

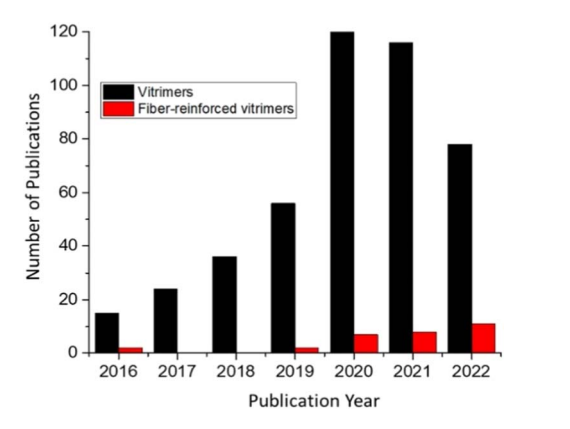


Fig. 2 From 2016 to January 2022, the number of published papers (according to Scopus, searching for fiber-reinforced composites and vitrimers in the title of the article).

reduce CO₂-emission and petroleum resources consumption. Several reports including reviews/mini-reviews have been published on the recyclability, surface welding, malleability, and mechanical properties of vitrimeric materials.³³⁻³⁶ However, none of them has covered the field of fiber-reinforced vitrimeric composites. The data in Fig. 2 clearly shows that the number of publications has been quickly increasing over the last couple of years. As a result, an updated literature review of self-healing vitrimer-based fiber-reinforced composites is attractive. Herein, we highlight and summarize dynamic fiber-reinforced composite materials including practical applications of this unique class of materials and future perspectives.

2. Characteristics of vitrimers

Viscosity of amorphous thermoplastics drops sharply above glass transition temperature (T_g) , and follows the William-Landel–Ferry (WLF) model between T_g and 100 °C above T_g , 37 as well as follows Arrhenius-type behaviour at higher temperatures.38 In case of semi-crystalline thermoplastics, the viscosity drops at $T_{\rm m}$ and follows Arrhenius temperature dependence as long as $T_{\rm m}$ is approximately 100 °C higher than its $T_{\rm g}$. In case of vitrimers, where viscosity is controlled by chemical exchange reaction,34 materials follow Arrhenius-type behaviour when significantly heated above $T_{\rm g}$, and thus, allows their processing without loss in network integrity. Moreover, along with T_g , a new temperature transition range (topology freezing transition temperature; $T_{\rm v}$); is introduced to identify the viscoelastic phase transition in vitrimers. Based on different measurement techniques and observations, a few definitions of T_{v} are reported, ranging from the original Leibler's investigation (where the effective viscosity crosses a value of 10¹² Pa s)³⁹ to the more recent suggestion of Winter and co-workers 40 (identifying the $T_{\rm v}$ point based on power-law relaxation of the modulus). Guan and co-workers suggested $T_{\rm v}$ as the crossover point where the Arrhenius high-temperature relaxation regime changes to the glassy dynamics.41 A number of techniques are used to identify $T_{\rm v}$, those include stress relaxation, ^{39,42} creep, ^{43,44} and fluorescence.45 Among them stress relaxation is the most accurate technique due to its independence from procedural parameters such as heating rate, however, due to a combination of thermal ramp with a standard tensile creep experiment, a nonisothermal creep testing is the quickest approach to determine the vitrification point.46

Based on the both, $T_{\rm g}$ and $T_{\rm v}$, vitrimers can be characterized into two pathways (Fig. 3). In a first case, $T_{\rm g}$ is situated below $T_{\rm v}$, whereas in another case $T_{\rm g}$ is situated well above the $T_{\rm v}$, however, in both the cases dynamic covalent bond exchange takes place at temperatures above the $T_{\rm g}$. The material behaves like a viscoelastic solid or rubbery material and thus follows either William–Landel–Ferry ($T_{\rm g} > T_{\rm v}$) or Arrhenius-type behaviour ($T_{\rm g} < T_{\rm v}$). As another feature, vitrimers exhibit great stress relaxation through bond exchanging at sufficiently high temperatures, despite the permanent network connectivity. The variation of relaxation time with changing temperatures follow Arrhenius relationship, similarly to the viscosity–temperature relationship described above.

RSC Advances Review

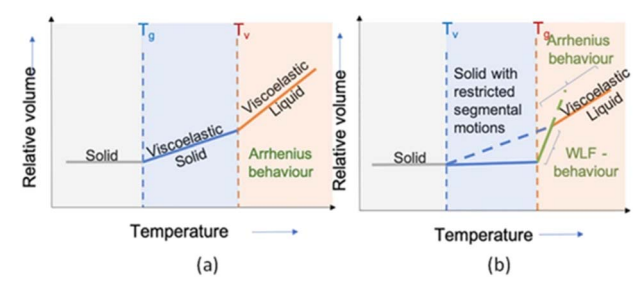


Fig. 3 Temperature dependent phase transitions of vitrimers. (a) $T_{\rm g}$ below $T_{\rm v}$ and (b) $T_{\rm g}$ above $T_{\rm v}$.

Recent work⁴⁷ in the context of dynamic covalent polymers indicates that besides the simple enthalpy (ΔH) , entropic (ΔS) contributions are of importance,⁴⁸⁻⁵⁰ especially when considering dynamic bond exchange in the condensed state.¹³ Examples of how thermodynamics of reversible bonds are changed in the solid state are provided *e.g.* by Barner-Kowolliks work, where a systematic impact of entropic effects in dissociation of dynamic bonds is described.^{49,51} Similar to known dynamic networks, there is a strong influence of the networks density, the nature of the crosslinking points on the association/dissociation of the individual bonds.⁵² This in turn is directly related to the overall stress recovery and the relation between bond exchange rates and stress–strain relationships.⁵³

Ran Ni and co-workers have analysed the role of entropy on the phase behaviour of the linker-mediated vitrimers, ⁵⁴ where the effect of linker concentration makes a huge impact reentering their gel–sol transition. The authors have observed that even at low temperature, the linker concentration determines the cross-linking degree of the vitrimers, which originates from the competition between the translational entropy of linkers and the conformational entropy of polymers (Fig. 4). Fig. 4B describes the plot for reaction constants K_2/K_1 (calculated by substituting the two metathesis reactions together) as a function of packing fraction of polymers (Φ_p) for different reaction sites (m) and chemical potential of cross-linker molecule (μ_C) with n=100.

Previous studies have focused on various vitrimer chemistries as well as the use of fillers55,56 or metal ions57,58 to improve the mechanical performance of vitrimer matrix. 59,60 It is widely known that adding fillers can expand the range of applications for these materials;61 however, it is unclear how filler addition affects the dynamic covalent bond exchanges as contradictory results are reported regarding the effect of filler on the vitrimer $T_{\rm v}$, creep, and stress relaxation. For instance, Yang and coworkers⁶² reported that adding filler reduces the T_v of the resulting vitrimer composite, whereas in contrast, a few reports present that addition of fillers increases the T_v of the composites.63,64 A similar kind of results were reported regarding the stress relaxation behavior, where in some reports the addition of fillers accelerates the stress relaxation,65 whereas, a slow stress relaxation was observed in other reports.^{66,67} The effect of incorporation of silica nanoparticles on stress relaxation and cross-link density recovery has been well analyzed.68 The functional groups (amine and hydroxyl) onto the surface of silica

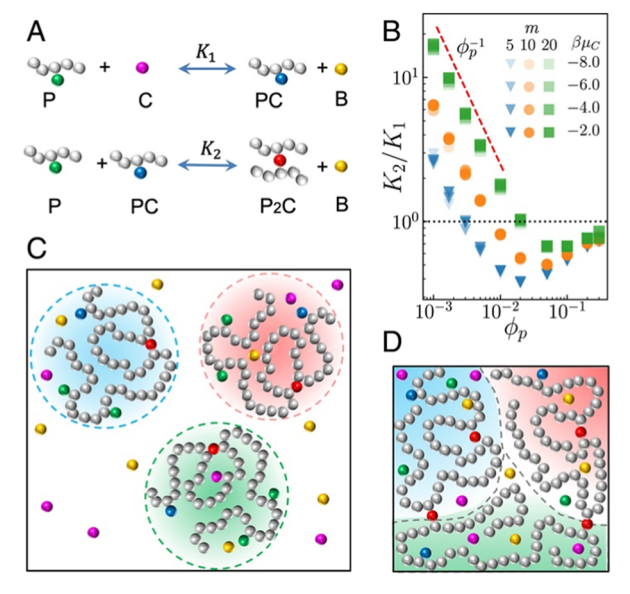


Fig. 4 Vitrimer model. (A) Illustration of the two-step metathesis reactions in the vitrimer system. (B) K_2/K_1 (reaction constants) as a function of $\Phi_{\rm p}$ ($\Phi_{\rm p}$: packing fraction of polymers) for different m (reaction sites) and $\mu_{\rm C}$ ($\mu_{\rm C}$; chemical potential of cross-linker molecule C) at n=100 and $\beta\mu_{\rm B}=-3$ ($\beta\mu_{\rm F}$) Boltzmann constant in terms of chemical potential of by-product molecules B in the system). (C and D) Illustration of the (C) heterogeneous dilute and (D) homogeneous dense systems of the vitrimers.⁵⁴

particles participate in reversible cyclic carbonate aminolysis reactions and transcarbamoylation exchange reactions, with polyhydroxyurethane network, respectively (Fig. 5). The study found that, the addition of functionalized nanofillers leads to a fast stress relaxation, however, after reprocessing, a loss in mechanical properties was observed. On the other hand, in case of nonreactive silica nanoparticles (without surface functional groups), the resulting network composite exhibits substantial increase in mechanical properties relative to pristine network, as indicated by the full recovery of rubbery plateau modulus after a reprocessing step. However, nanofillers restrict the network matrix mobility, thus leading towards a slow rate of network rearrangement. The findings are in agreement with previous reports, where researchers also observed a fast stress

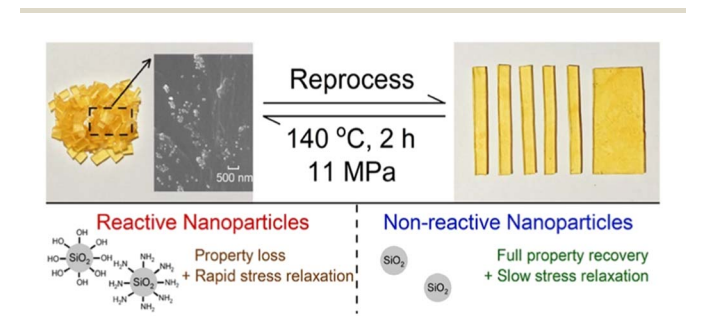


Fig. 5 Reprocessable polyhydroxyurethane network nanocomposites using silica nanoparticles with different surface functionalities as reinforcing fillers.⁶⁸

Review

relaxation when there is a dynamic chemistry between polymer matrix and functional groups decorated silica nanoparticles.^{69,70}

Hayashi *et al.*⁷¹ prepared the vitrimer-like materials operated through *trans-N*-alkylation of quaternized pyridine groups. The composite sample was prepared by incorporation of silica nanoparticles with hydrophobic surfaces at the silica volume fraction range (Φ_P) from 0.06 to 0.36.

The modulus and toughness at room temperature increased with an increase in $\Phi_{\rm P}$, whereas the bond exchange nature at high temperatures was sustained, according to the stress-relaxation tests. Notably, with an increase of $\Phi_{\rm P}$, the average relaxation time ($\langle \tau^* \rangle$) was increased and the model analysis based on the Kohlrausch–Williams–Watts (KWW) function revealed that the distribution of the relaxation time was enlarged (*i.e.*, β in the KWW function was decreased). These changes were attributed to the formation of bound rubber phase as well as the strong adhesion between the SNP and matrix (Fig. 6). Hubbard and co-workers⁴⁶ also demonstrated that by adjusting the filler content, composition, and dispersion quality, it is feasible to build composites with tailorable $T_{\rm v}$, strength, and processability.

A similar effect can be assumed for dynamic bonding equilibria in fiber-reinforced vitrimers, where the interaction between filler and network matrix can play a significant role on covalent bond rearrangement process. In a very recent study, Gresil and co-workers have studies the instability of the crack propagation for vitrimer/CFRP composites.⁷² The authors observed that laminates within the vitrimer matrix acquired a higher load than pure epoxy CFRP to propagate the crack, especially when interface adhesion between vitrimer matrix and the carbon fiber is strong. While considering the energy at crack propagation, fracture toughness for fibers/vitrimer was increased by ~63%, with respect to epoxy/CF, confirming that apart from toughness of the matrix, interface and the interphase between matrix and the fibre play a very important role on fracture toughness.

To process the fiber-reinforced vitrimer composites, it is essentially important to study the rheological behavior of vitrimer matrix. The reports found that regrading curing kinetics both the traditional thermosets as well as vitrimer matrix displays two distinct zones. Both resin viscosities in the first region were either stable or slowly decreased with rising

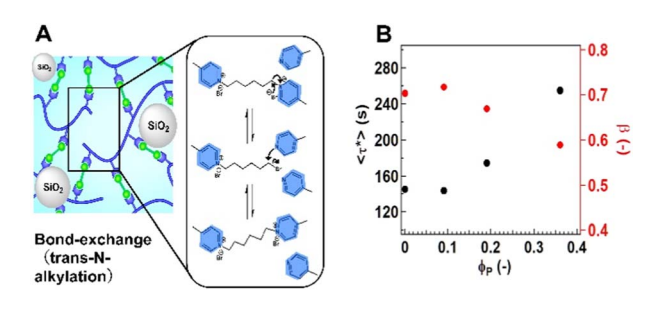


Fig. 6 (A) Schematic representation of the vitrimer-like composite with silica-nano particles. (B) Variation of $(\langle \tau^* \rangle)$ and β as a function of Φ_P (see the explanation of $\langle \tau^* \rangle$ and $\langle \beta \rangle$ in the main text). From ref. 71 produced/adapted by permission of Springer Nature.

temperature. However, in case of thermosets the viscosity grows exponentially over time in the second zone at higher temperatures, whereas, vitrimer matrix displays a slow curing process, and thus offer a wider temperature window for pultruded fiber composites.⁷³ Furthermore, for better fiber impregnation and minimal void content, vitrimeric resins can be heated at any stage of production.⁷⁴

Therefore, while designing the vitrimeric composites, researchers need a special attention regarding dispersion quality of fillers, the strength of the filler/matrix interface, filler surface chemistry, filler geometry (lateral νs . thickness variation), as well as different methods of T_{ν} identification.

3. Chemistries used to develop vitrimer composites

Thanks to a collection of bond exchangeable chemistries, the family of covalent adaptable networks (CANs) plays a gallant step in bridging the gap between thermoplastics and thermosets. Based on their dynamic nature, several exchangeable chemistries have been used for the preparation of vitrimeric materials, where the most popular chemistries include; transesterification, transcarbamoylation, disulfide exchange, transamination of vinylogous urethanes, transalkylation of triazolium salts, and amine imine exchange (Schiff Chemistry). In fact, some in the above examples (i.e., transcarbamoylation, transalkylation of triazolium salts, amine imine exchange) do not result in "true" vitrimers, since these bond exchange reactions progress in a dissociative pathway. In these bond exchange reaction, the bond dissociation and re-association occurs in a distinct separated steps, and thus the network materials with such bond exchange mechanism cannot be classified as vitrimers. On the other hand, due to the consequence of either fast bond reformation or the large equilibrium constant in favour of the associated state within high temperatures, the "apparent" network connectivity can be maintained, similarly to vitrimers. To distinguish them from true vitrimers, these materials are called vitrimer-like. In the present review, we do not classify these two strictly, i.e., either true vitrimers or vitrimer-like materials, to follow the original terminology given in each reference. The readers must consider the origin of the exchange reaction carefully to classify the materials. Table 1 summarized some features of reported materials with fiber-type fillers, including mechanical properties, healing efficiencies, and healing conditions.

3.1 Transesterification reactions

Transesterification-chemistry is one of the most studied chemical reactions used for the development of vitrimeric materials.⁷⁵ Qi and co-workers have performed an ethylene glycol and epoxy based transesterification reaction for the recycling of CFRP composites.⁷⁶ The authors dissolved the prepared vitrimers in an alcoholic solvent at 160–180 °C, a temperature below the thermal degradation temperature of carbon fibers (~500 °C)⁷⁷ and the epoxy matrix (~350 °C).⁷⁸ Slight heating of the solvent led to the evaporation of alcohol

Table 1 The self-healing properties of FRP materials based on dynamic covalent bonds. The tensile strength, healing efficiency, and healing conditions relevant to each are also listed

Forms (T,) Healing conditions Healing efficiency 57 180 °C, 4 h			Glass transition	Glass transition Topology freezing			Tensile strength	
Carbon fiber/bidirectional 30 57 180 °C, 4 h 97% modulus, 95% tensile strength Carbon fiber/bidirectional 34 72 200 °C, 3 h 100% shape memory properties Carbon fiber/bidin weave 50 118 160 °C, 1 h, and 30 min Adhesive properties (lap-shear test)- Carbon fiber/plain weave 72 94 180 °C, 1 h, and 30 min Adhesive properties (lap-shear test)- Carbon fiber/plain weave 72 94 180 °C, 1 h, and 30 min Adhesive properties (lap-shear test)- Carbon fiber/plain weave 72 94 180 °C, 1 h, and 30 min Adhesive properties (lap-shear test)- Carbon fiber/plain weave 32 6 140 °C, 12 h 73% tensile strength Carbon fiber/plain weave 13 54 150 °C, 15 min 90% tensile strength Carbon fiber/plain weave 147 171 200 °C, 2 h 95% tensile strength Carbon fiber/plain weave 130 130 140 °C, 12 h 95% tensile strength Carbon fiber/plain weave 13 171 200 °C, 2 h 95% tensile strength Carbon fiber/plain weave 36 200 °C, 2 h 9	Mechanism	Fiber/fiber direction	$T_{\rm g} (^{\circ}{ m C})$	temperature $(T_{\rm v})$	Healing conditions	Healing efficiency	(measured at 25 °C)	Ref.
Carbon fiber/bidirectional 34 72 200 °C, 3 h — 100% shape memory properties Garbon fiber/woven 66 — 160 °C, 3 h 100% shape memory properties Garbon fiber/woven 50 118 160 °C, 1 h, and 30 min Adhesive properties (lap-shear test) Garbon fiber/woven 45 — 180 °C, 1 h 100% shape memory properties Garbon fiber/bidirectional 57 56 190 °C, 3 h 38% strain at failure Garbon fiber/bidirectional 150 — 140 °C, 12 h 98% strain at failure Garbon fiber/plain weave 120 — 140 °C, 12 h 98% strain at failure Garbon fiber/plain weave 149 80 100 °C, 12 h 98% strains strength Garbon fiber/plain weave 149 80 100 °C, 12 h 98% strains strength Garbon fiber/plain weave 147 171 200 °C, 2 h 98% strains strength Garbon fiber/plain weave 132 52 180 °C, 4 h 97% strains strength Garbon fiber/plain weave 130 70 180 °C, 2 h 98% strain	Transesterification	Carbon fiber/bidirectional	30	57	180 °C, 4 h	97% modulus, 95% tensile strength	06	92
Carbon fiber/woven 66 — 160 °C, 3 h 100% shape memory properties Gass fiber/plain weave 50 118 160 °C, 1 h, and 30 min Adhesive properties (lap-shear test)- Carbon fiber/woven 44 97 180 °C, 1 h 100% reversed fatigue Carbon fiber/plain weave 72 94 180 °C, 3 min 100% reversed fatigue Carbon fiber/plain weave 75 64 180 °C, 3 min 100% reversed fatigue Carbon fiber/plain weave 32 54 180 °C, 3 min 100% respirable remony properties Carbon fiber/plain weave 32 54 180 °C, 3 min 100% respirable remony properties Carbon fiber/plain weave 32 54 180 °C, 15 min 90% tensile strength Carbon fiber/plain weave 32 54 180 °C, 15 min 90% tensile strength Carbon fiber/plain weave 32 52 40 °C, 12 h 95% tensile strength Carbon fiber/plain weave 32 52 40 °C, 12 h 95% tensile strength Carbon fiber/plain weave 33 56 76 40 °C, 12 h		Carbon fiber/bidirectional	34	72	200 °C, 3 h		50–80	79
Glass fiber/plain weave 50 118 160 °C, 1 h, and 30 min Adhesive properties (Jap-shear test) Carbon fiber/woven 44 97 180 °C, 1 h 100% shape memory properties Carbon fiber/plain weave 72 94 180 °C, 1 h 73% tensile strength Carbon fiber/plain weave 72 94 180 °C, 30 min 100% shape memory properties Carbon fiber/plain weave 32 54 150 °C, 12 h 9% tensile strength Garbon fiber/plain weave 149 80 200 °C, 12 h 9% tensile strength Garbon fiber/plain weave 149 80 200 °C, 12 h 9% tensile strength Carbon fiber/plain weave 140 80 200 °C, 12 h 9% tensile strength Carbon fiber/plain weave 130 -13 200 °C, 2 h 9% tensile strength Carbon fiber/plain weave 130 70 40 9% tensile strength Carbon fiber/plain weave 130 76 200 °C, 2 h 9% tensile strength Carbon fiber/plain weave 130 76 200 °C, 2 h 9% tensile strength		Carbon fiber/woven	99	1	160 °C, 3 h	100% shape memory properties	356	80
Carbon fiber/woven 44 97 180 °C, 1h 100% Carbon fiber/unidirectional 45 — 180 °C, 1h 73% tensile strength Carbon fiber/unidirectional 72 94 180 °C, 3 min 100% shape memory properties Carbon fiber/plain weave 72 94 180 °C, 3 min 100% shape memory properties Carbon fiber/plain weave 32 54 150 °C, 12 h 90% tensile strength Carbon fiber/plain weave 149 80 200 °C, 6 h 90% tensile strength Carbon fiber/plain weave 147 171 200 °C, 6 h 90% tensile strength Carbon fiber/plain weave 130 -13 200 °C, 1h 89% tensile strength Carbon fiber/plain weave 130 76 200 °C, 2h 95% tensile strength Carbon fiber/plain weave 130 76 200 °C, 2h 89% tensile strength Carbon fiber/plain weave 131 101 180 °C, 1h 89% tensile strength Carbon fiber/plain weave 13 101 100 °C, 2h 87% elongation at break <		Glass fiber/plain weave	50	118	160 °C, 1 h, and 30 mi	n Adhesive properties (lap-shear test)-	522	81
Carbon fiber/woven 44 97 180 °C, 1 h 100% reversed fatigue Carbon fiber/midirectional 45 — 94 180 °C, 4 h 73% ensile strength Carbon fiber/plain weave 32 54 190 °C, 3 h 88% strain at failure Carbon fiber/plain weave 32 54 190 °C, 12 h 99% tensile strength Carbon fiber/plain weave 32 54 150 °C, 12 h 99% tensile strength Garbon fiber/plain weave 147 171 200 °C, 2 h 95% tensile strength Carbon fiber/plain weave 147 171 200 °C, 2 h 95% tensile strength Carbon fiber/plain weave 130 -13 200 °C, 2 h 95% tensile strength Carbon fiber/midirectional 130 -13 200 °C, 2 h 95% tensile strength Carbon fiber/minexe 33 56 200 °C, 2 h 87% oung's modulus Carbon fiber/minexe 33 56 200 °C, 2 h 87% enoigation at break Carbon fiber/plain weave 83 56 200 °C, 2 h 87% enoigation at break <t< td=""><td></td><td></td><td></td><td></td><td></td><td>100%</td><td></td><td></td></t<>						100%		
Carbon fiber/unidirectional 45 — 180 °C, 4 h 73% tensile strength Carbon fiber/plain weave 72 94 180 °C, 30 min 100% shape memory properties Carbon fiber/plain weave 32 54 140 °C, 12 h 90% tensile strength Carbon fiber/plain weave 32 54 150 °C, 15 min 98% tensile strength Carbon fiber/plain weave 149 80 200 °C, 6 h 100% tensile strength Carbon fiber/plain weave 147 171 200 °C, 6 h 97% interlaminar shear strength Carbon fiber/plain weave 130 -13 200 °C, 20 s 97% interlaminar shear strength Carbon fiber/plain weave 130 70 180 °C, 12 h 89% tensile strength Carbon fiber/plain weave 13 50 200 °C, 20 s 97% interlaminar shear strength Carbon fiber/plain weave 13 50 140 °C, 12 h 89% tensile strength Carbon fiber/plain weave 13 50 200 °C, 2 h 87% elongation at break Carbon fiber/plain weave 13 101 110 °C, 2 h <td< td=""><td></td><td>Carbon fiber/woven</td><td>44</td><td>26</td><td>180 °C, 1 h</td><td>100% reversed fatigue</td><td>449</td><td>82</td></td<>		Carbon fiber/woven	44	26	180 °C, 1 h	100% reversed fatigue	449	82
Carbon fiber/plain weave 72 94 180 °C, 30 min 100% shape memory properties Carbon fiber/pidirectional 57 76 190 °C, 31h 88% strain at failure Carbon fiber/woven 32 54 150 °C, 12 min 98% tensile strength Carbon fiber/plain weave 149 80 200 °C, 6 h 100% reshaping Carbon fiber/plain weave 147 171 200 °C, 2 h 95% tensile strength Carbon fiber/plain weave 147 171 200 °C, 2 h 95% tensile strength Carbon fiber/plain weave 132 52 180 °C, 2 h 95% tensile strength Carbon fiber/plain weave 132 52 200 °C, 2 h 89% tensile strength Carbon fiber/plain weave 130 76 200 °C, 2 h 89% tensile strength Carbon fiber/plain weave 13 76 200 °C, 2 h 89% tensile strength Carbon fiber/plain weave 131 101 180 °C, 1 h 87% clongation at break Carbon fiber/plain weave 131 101 180 °C, 1 h 87% clongation at break <		Carbon fiber/unidirectional	45	I	180 °C, 4 h	73% tensile strength	41.66	83
Carbon fiber/bidirectional 57 76 190 °C, 3 h 88% strain at failure Carbon fiber/woven 150 — 140 °C, 12 h 90% tensile strength Carbon fiber/plain weave 132 54 150 °C, 15 min 90% tensile strength Carbon fiber/plain weave 147 171 200 °C, 6 h 92% tensile strength Carbon fiber/plain weave 147 171 200 °C, 2 h 95% tensile strength Carbon fiber/plain weave 130 —13 200 °C, 2 h 95% tensile strength Carbon fiber/plain weave 132 52 180 °C, 14 h 85% elongation at break Carbon fiber/plain weave 83 56 200 °C, 2 h 85% elongation at break Carbon fiber/plain weave 131 101 180 °C, 1 h 87% elongation at break Carbon fiber/plain weave 70 85 200 °C, 2 h 87% elongation at break Carbon fiber/plain weave 131 101 180 °C, 1 h 87% elongation at break Carbon fiber/plain weave 131 101 85 100 °C, 2 h 80% tensile s		Carbon fiber/plain weave	72	94	180 °C, 30 min	100% shape memory properties	465	84
Carbon fiber/blain weave 150 — 140 °C, 12 h 90% tensile strength Carbon fiber/plain weave 149 54 150 °C, 15 min 98% tensile strength Carbon fiber/plain weave 149 80 200 °C, 6 h 100% reshaping Carbon fiber/plain weave 147 171 200 °C, 2 h 95% tensile strength Carbon fiber/plain weave 130 -13 200 °C, 2 h 97% tensile strength Carbon fiber/plain weave 132 52 180 °C, 4 h 89% tensile strength Carbon fiber/plain weave 136 76 200 °C, 2 h 87% elongation at break Carbon fiber/plain weave 131 101 180 °C, 1 h 87% elongation at break Carbon fiber/plain weave 131 101 180 °C, 1 h 87% elongation at break Carbon fiber/plain weave 131 101 180 °C, 1 h 87% elongation at break Carbon fiber/plain weave 131 101 180 °C, 2 h 87% elongation at break Carbon fiber/plain weave 131 101 100 °C, 2 h 60% tensile strength <td></td> <td>Carbon fiber/bidirectional</td> <td>57</td> <td>92</td> <td>190 °C, 3 h</td> <td>88% strain at failure</td> <td>5.6</td> <td>82</td>		Carbon fiber/bidirectional	57	92	190 °C, 3 h	88% strain at failure	5.6	82
Carbon fiber/plain weave 32 54 150 °C, 15 min 98% tensile strength Class fiber/plain weave 149 80 200 °C, 6 h 100% reshaping Carbon fiber/plain weave 147 171 200 °C, 2 h 95% tensile strength Carbon fiber/plain weave 147 171 200 °C, 2 h 95% tensile strength Carbon fiber/plain weave 132 52 95% tensile strength Carbon fiber/plain weave 96 76 200 °C, 2 h 89% tensile strength Carbon fiber/plain weave 96 76 200 °C, 2 h 85% elongation at break Carbon fiber/plain weave 131 101 180 °C, 1 h 85% elongation at break Carbon fiber/plain weave 13 56 200 °C, 2 h 87% elongation at break Carbon fiber/plain weave 13 101 180 °C, 1 h 88% tensile strength Carbon fiber/plain weave 150 85 140 °C, 10 min 87% elongation at break Carbon fiber/plain weave 150 85 100 °C, 2 h 60% tensile strength Carbon fiber/p		Carbon fiber/woven	150	I	140 °C, 12 h	90% tensile strength	457	98
Glass fiber/plain weave 149 80 200 °C, 6 h 100% reshaping Carbon fiber/plain weave 147 128 180 °C, 4 h 92% tensile strength Carbon fiber/plain weave 147 171 200 °C, 2 h 97% tensile strength Carbon fiber/plain weave 170 70 40 °C, 12 h 89% tensile strength Carbon fiber/plain weave 182 52 180 °C, 4 h 89% tensile strength Carbon fiber/plain weave 83 56 200 °C, 2 h 87% elongation at break Carbon fiber/plain weave 70 85 140 °C, 1 h 87% elongation at break Carbon fiber/plain weave 70 85 200 °C, 2 h 87% elongation at break Carbon fiber/plain weave 131 101 180 °C, 1 h 88% tensile strength Carbon fiber/plain weave 130 55 200 °C, 2 h 87% elongation at break Carbon fiber/plain weave 131 101 140 °C, 1 h 88% tensile strength Carbon fiber/plain ectional 74		Carbon fiber/plain weave	32	54	150 °C, 15 min	98% tensile strength	127	87
Carbon fiber/bidirectional 116 128 180 °C, 4 h 92% tensile strength Carbon fiber/plain weave 47 171 200 °C, 2 h 95% tensile strength Carbon fiber/plain weave 132 52 97% interlaminar shear strength Carbon fiber/plain weave 96 76 200 °C, 2 h 89% tensile strength Carbon fiber/plain weave 96 76 200 °C, 2 h 87% elongation at break Carbon fiber/plain weave 70 85 140 °C, 10 min 37% elongation at break Carbon fiber/plain weave 70 85 140 °C, 10 min 37% elongation at break Carbon fiber/plain weave 131 101 180 °C, 1h 88% tensile strength Carbon fiber/plain weave 131 101 180 °C, 1h 88% tensile strength Carbon fiber/plain weave 150 85 170 °C, 4h 60% tensile strength Glass fiber/bidirectional 74 — 150 °C, 5min 60% tensile strength Glass fiber/bidirectional 10 125 160 °C, 5min 76% young's modulus <td< td=""><td>Disulfide exchange</td><td>Glass fiber/plain weave</td><td>149</td><td>80</td><td>200 °C, 6 h</td><td>100% reshaping</td><td>451</td><td>88</td></td<>	Disulfide exchange	Glass fiber/plain weave	149	80	200 °C, 6 h	100% reshaping	451	88
Carbon fiber/plain weave 147 171 200 °C, 2 b 95% tensile strength Carbon fiber/bidirectional 130 -13 200 °C, 2 0 s 97% interlaminar shear strength Carbon fiber/bidirectional 170 70 70 40 °C, 12 h 89% tensile strength Carbon fiber/moven 132 52 180 °C, 4 h 84% young's modulus Carbon fiber/plain weave 96 76 200 °C, 2 h 87% elongation at break Carbon fiber/plain weave 131 101 180 °C, 1 h 87% elongation at break Carbon fiber/plain weave 131 101 180 °C, 1 h 87% elongation at break Carbon fiber/plain weave 131 101 180 °C, 1 h 88% tensile strength Carbon fiber/midirectional 80 35 200 °C, 2 h 60% tensile strength Poplass fiber/E-type 200 85 140 °C, 4 h 60% tensile strength Glass fiber/E-type 200 85 140 °C, 5 min 60% tensile strength Glass fiber/bidirectional 74 60% tensile strength 76% young's modulus		Carbon fiber/bidirectional	116	128	180 °C, 4 h	92% tensile strength	33	88
Carbon fiber/bidirectional 130 -13 200 °C, 20 s 97% interlaminar shear strength Carbon fiber/woven 170 70 40 °C, 12 h 89% tensile strength Carbon fiber/woven 132 52 180 °C, 4 h 84% young's modulus Carbon fiber/plain weave 96 76 200 °C, 2 h 87% elongation at break Carbon fiber/plain weave 83 56 200 °C, 2 h 87% elongation at break Carbon fiber/plain weave 131 101 180 °C, 1 h 88% tensile strength Carbon fiber/plain weave 130 35 200 °C, 2 h 60% tensile strength Carbon fiber/unidirectional 80 35 170 °C, 4 h 60% tensile strength Glass fiber/bidirectional 74 — 150 °C, 2 h 60% tensile strength Glass fiber/bidirectional 74 — 150 °C, 2 h 60% tensile strength Glass fiber/bidirectional 74 — 150 °C, 2 h 60% tensile strength Glass fiber/bidirectional 74 — 150 °C, 2 h 60% tensile strength		Carbon fiber/plain weave	147	171	200 °C, 2 h	95% tensile strength	334.5	90
Carbon fiber/unidirectional 170 70 40 °C, 12 h 89% tensile strength Carbon fiber/woven 132 52 180 °C, 4 h 84% young's modulus Carbon fiber/plain weave 96 76 200 °C, 2 h 85% elongation at break Carbon fiber/plain weave 70 85 140 °C, 10 min 37% elongation at break Carbon fiber/plain weave 131 101 180 °C, 1 h 88% tensile strength Carbon fiber/plain weave 130 55 200 °C, 2 h 60% tensile strength Carbon fiber/plain weave 130 35 170 °C, 4 h 60% tensile strength Carbon fiber/bridirectional 74 — 150 °C, 5 min 60% tensile strength Glass fiber/bridirectional 74 — 150 °C, 55 min 60% tensile strength Glass fiber/bridirectional 74 — 150 °C, 55 min 76% young's modulus Garbon fiber/bridirectional 85 150 °C, 55 min 74.5% tensile strain		Carbon fiber/bidirectional	130	-13	200 °C, 20 s	97% interlaminar shear strength	557	91
Carbon fiber/woven 132 52 180 °C, 4 h 84% young's modulus Carbon fiber/plain weave 96 76 200 °C, 2 h 85% elongation at break Carbon fiber/plain weave 70 85 200 °C, 2 h 87% elongation at break Carbon fiber/plain weave 131 101 180 °C, 1 h 88% tensile strength Carbon fiber/plain weave 131 101 200 °C, 2 h 60% tensile strength Carbon fiber/plain weave 80 35 170 °C, 4 h 60% tensile strength Unidirectional 80 85 140 °C, 30 min 60% tensile strength Glass fiber/beirectional 74 — 150 °C, 55 min 150 °C, 55 min 76% young's modulus Glass fiber/bidirectional 110 125 150 °C, 55 min 63% fracture toughness Carbon fiber/plain weave 145 °C, 2h 74.5% tensile strain		Carbon fiber/unidirectional	170	70	40 °C, 12 h	89% tensile strength	873	92
Carbon fiber/plain weave 96 76 200 °C, 2 h 85% elongation at break Carbon fiber/plain weave 70 85 140 °C, 10 min 37% elongation at break Carbon fiber/plain weave 131 101 180 °C, 1h 88% tensile strength Carbon fiber/plain weave 131 101 200 °C, 2 h 60% tensile strength Carbon fiber/plain weave 80 35 170 °C, 4 h 60% tensile strength Poplar wood fibers/ 80 85 140 °C, 30 min 60% tensile strength I class fiber/E-type 200 85 140 °C, 30 min 60% tensile strength Glass fiber/bidirectional 74 — 150 °C, 55 min 76% young's modulus Garbon fiber/bidirectional 85 110 125 150 °C, 55 min 76% young's modulus Carbon fiber/plain weave 145 65 145 °C, 2 h 74.5% tensile strain	Imine exchange	Carbon fiber/woven	132	52	180 °C, 4 h	84% young's modulus	571	93
Carbon fiber/plain weave 83 56 200 °C, 2 h 87% elongation at break Carbon fiber/plain weave 70 85 140 °C, 10 min 37% elongation at break Carbon fiber/plain weave 131 101 180 °C, 1h 88% tensile strength Carbon fiber/plain weave 150 55 200 °C, 2 h 60% tensile strength Poplar wood fibers/ 80 35 170 °C, 4 h 60% tensile strength unidirectional 200 85 140 °C, 30 min 60% tensile strength Glass fiber/bidirectional 74 — 150 °C, 55 min 76% young's modulus Glass fiber/bidirectional 110 125 150 °C, 55 min 76% young's modulus Carbon fiber/plain weave 145 65 160 °C, 2 h 74.5% tensile strain		Carbon fiber/plain weave	96	92	200 °C, 2 h	85% elongation at break	622	94
Carbon fiber/plain weave 70 85 140 °C, 10 min 37% elongation at break Carbon fiber/plain weave 131 101 180 °C, 1h 88% tensile strength Carbon fiber/unidirectional 150 55 200 °C, 2 h 60% tensile strength Poplar wood fibers/ 80 35 170 °C, 4 h 60% tensile strength unidirectional 200 85 140 °C, 30 min 60% tensile strength Glass fiber/bidirectional 74 — 150 °C, 55 min 76% young's modulus Glass fiber/bidirectional 110 125 150 °C, 55 min 76% young's modulus Carbon fiber/plain weave 145 65 160 °C, 2 h 74.5% tensile strain		Carbon fiber/plain weave	83	56	200 °C, 2 h	87% elongation at break	584	94
Carbon fiber/plain weave 131 101 180 °C, 1 h 88% tensile strength Carbon fiber/unidirectional 150 55 200 °C, 2 h 60% tensile strength Poplar wood fibers/ 80 35 170 °C, 4 h 60% tensile strength unidirectional 200 85 140 °C, 30 min 60% tensile strength Glass fiber/beitrectional 74 — 150 °C, 55 min 83% elongation at failure Glass fiber/bidirectional 110 125 150 °C, 55 min 76% young's modulus Carbon fiber/plain weave 145 65 160 °C, 2 h 74.5% tensile strain		Carbon fiber/plain weave	70	85	140 °C, 10 min	37% elongation at break	449	29
Carbon fiber/unidirectional 150 55 200 °C, 2 h 60% tensile strength Poplar wood fibers/ 80 35 170 °C, 4 h 60% tensile strength unidirectional 200 85 140 °C, 30 min 60% tensile strength Glass fiber/bidirectional 74 — 150 °C, 55 min 83% elongation at failure Glass fiber/bidirectional 110 125 150 °C, 55 min 76% young's modulus Carbon fiber/plain weave 145 65 160 °C, 2 h 74.5% tensile strain		Carbon fiber/plain weave	131	101	180 °C, 1 h	88% tensile strength	82	95
Poplar wood fibers/ 80 35 170 °C, 4 h 60% tensile strength unidirectional 200 85 140 °C, 30 min 60% tensile strength Glass fiber/bidirectional 74 — 150 °C, 55 min 83% elongation at failure Glass fiber/bidirectional 110 125 150 °C, 55 min 76% young's modulus Carbon fiber/plain weave 185 110 145 °C, 8 h 63% fracture toughness Carbon fiber/plain weave 145 65 160 °C, 2 h 74.5% tensile strain		Carbon fiber/unidirectional	150	55	200 °C, 2 h	60% tensile strength	64	96
unidirectional Glass fiber/E-type Glass fiber/bidirectional Glass fiber/bidirectional T4 — 150 °C, 55 min Glass fiber/bidirectional T10 125 110 145 °C, 8 h Garbon fiber/unidirectional S5 110 145 °C, 8 h Garbon fiber/plain weave T45 65 min T6% young's modulus T78		Poplar wood fibers/	80	35	170 °C, 4 h	60% tensile strength	21	97
Glass fiber/E-type20085140 °C, 30 min60% tensile strengthGlass fiber/bidirectional74—150 °C, 55 min83% elongation at failureGlass fiber/bidirectional110125150 °C, 55 min76% young's modulusCarbon fiber/unidirectional85110145 °C, 8 h63% fracture toughnessCarbon fiber/plain weave14565160 °C, 2 h74.5% tensile strain		unidirectional						
Glass fiber/bidirectional 74 — 150 °C, 55 min 83% elongation at failure Glass fiber/bidirectional 110 125 150 °C, 55 min 76% young's modulus Carbon fiber/unidirectional 85 110 145 °C, 8 h 63% fracture toughness Carbon fiber/plain weave 145 65 160 °C, 2 h 74.5% tensile strain	Other exchange	Glass fiber/E-type	200	85	140 °C, 30 min	60% tensile strength	55	86
110 125 150 °C, 55 min 76% young's modulus 85 110 145 °C, 8 h 63% fracture toughness 145 65 160 °C, 2 h 74.5% tensile strain	reactions	Glass fiber/bidirectional	74	1	150 °C, 55 min	83% elongation at failure	939	66
85 110 145 °C, 8 h 63% fracture toughness 145 65 160 °C, 2 h 74.5% tensile strain		Glass fiber/bidirectional	110	125	150 °C, 55 min	76% young's modulus	64	100
145 65 160 °C, 2 h $74.5%$ tensile strain		Carbon fiber/unidirectional	85	110	145 °C, 8 h	63% fracture toughness	821	72
		Carbon fiber/plain weave	145	65	160 °C, 2 h	74.5% tensile strain	91	101

200 °C).

Review

and the thermoset was repolymerized displaying similar thermomechanical properties as initial polymer with almost 100% recovery of polymer and CFRP. Stress-strain curves confirm the good consistency including a full recovery of mechanical properties for the repaired and recycled fibers. Further, Long and co-workers⁷⁹ have developed FRPs (fiber reinforced composites) using a transesterification-based exchangeable epoxy network, initially reported by Leibler and co-workers.29 The polymeric material shows rubbery behavior at room temperature with 2.8 MPa and 3.8 MPa tensile strength and Young's modulus, respectively. Fabricated FRP composites therefrom demonstrate exceptional mechanical properties, with 50-80 MPa (tensile strength) and a 3-8 GPa Young's modulus, respectively. In addition, anhydride-derived carbon fiber reinforced epoxy vitrimers with good rigidity and recyclability were reported.80 Initially, a tertiary amine-containing prepolymer was prepared by reaction of ethylenediamine with bisphenol A, and the prepared pre-polymer was further reacted with glutaric anhydride (GA) to develop transesterification based exchange network. A hand lay-up method was used to prepare vitrimer composites consisting of three layers of carbon fiber fabrics. The reported composites demonstrate good tensile strength due to the presence of abundant -OH groups of the polymer matrix (non-stoichiometrically anhydride cured epoxy), able to facilitate an interfacial interaction with fibers. Due to dynamic transesterification, the vitrimeric matrix exhibits good stress relaxation behavior (150 °C) able to retain the cross-linked network along with release in internal stress. The epoxy matrix exhibits a low glass transition temperature $(T_g; 66)$, owing to the presence of glutaric anhydride. However, when glutaric anhydride was replaced by rigid nadic anhydride (as rigid curing agent), the resulting epoxy exhibits higher T_{σ} (95 ° C) and tensile strength (58 MPa vs. 50.5 MPa for glutaric anhydride based epoxy); however, due to rigid structure nadic anhydride restricts the polymer chains mobility, thus, an increase in relaxation time was observed (3800 s vs. 1160 s at

Defects and size limitations often force engineers to design multiple parts separately and further assemble them as per application requirements. However, it is almost impossible to reprocess the cured thermosets, thus, their welding is a big challenge. Tournilhac and co-workers have studied the multiple welding of carbon fiber reinforced vitrimer composites having more than 50 vol% reinforcing fibers, prepared using resin transfer molding (RTM).⁸¹ As the resin demonstrates a lower viscosity (<1 Pa s) at 50 °C, it was transferred under these conditions, and later cured at 120 °C for 4 h and 160 °C for 3 h. The reported epoxy vitrimer also shows exceptional adhesive properties, where poly(ethylene terephthalate (PET)) sheets were successfully connected using the prepared adhesive (160 °C; 90 min).

Fiber-reinforced vitrimer composites can be designed for reversing the fatigue-induced damage by heating it above T_v . Kamble and co-workers developed an epoxy vitrimer from diglycidyl ether of bisphenol-A (DGEBA) and adipic acid (AA) in the presence of 1,5,7-triazabicyclo [4,4,0] dec-5-ene (TBD) as a catalyst.⁸² The DGEBA/AA vitrimer system observed failure

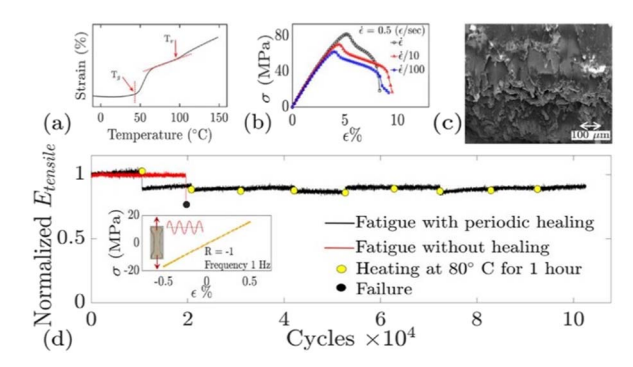


Fig. 7 Reversing fatigue damage in vitrimers by repeated doses of healing. (a) Strain measured in a dilatometric experiment with heating rate of 2.5 K min⁻¹ at stress of 25 kPa. (b) Static tensile testing at room temperature and for three different strain rates. (c) Typical fracture surface image of the failed vitrimer. (d) Fatigue test showing normalized modulus vs. the number of cycles of fatigue loading.⁸²

 \sim 20 000 number of cycles, where modulus drops sharply as the sample fractures. In contrast, when the healing treatment was performed every 10 000 cycles, no indication of failure was observed even after 100 000 cycles (Fig. 7a-c). Therefore, fatigue failure in the vitrimer can be periodically reverse (due to repairing) by repeated doses of healing treatments using covalent adaptive network exchanges. However, compared to the pristine vitrimer (80 °C), authors used a higher healing temperature for the vCFRP (~150 °C), where researchers assumed that higher temperature is helpful not only for vitrimer flow but also helpful for healing the delamination at fibermatrix interphase (Fig. 7d). However, no systematic analysis was performed to prove the delamination healing. The effect of temperature, time, and resin content on the strength of the vitrimeric matrix and its composites must be investigated to provide considerable interface repair.

Zhao and co-workers⁸³ created epoxy vitrimers based on DGEBA and then treated them with glutaric anhydride in the presence of zinc acetylacetonate catalyst. At 180 °C, with a curing period of 4 hours and a resin concentration of 10.71%, the reported epoxy vitrimer displays outstanding interface bonding strength. The material's interface strength was examined using a tensile test and a single lap test, with the connection method yielding a tensile strength of 30.12 MPa on average.

With advancements in the realm of "green chemistry," developing non-petroleum-based matrices for manufacturing of self-healing FRPs would be highly valuable. In a recent study, Chen and co-workers have developed carbon fiber reinforced composites using a degradable epoxidized menthane diamine-adipic acid (EMDA-AA) matrix, obtained from bio-based menthane diamine and adipic acid. Due to autocatalysis of tertiary amines in the EMDA-AA vitrimer, the vitrimer network demonstrates topological rearrangement *via* dynamic transesterification reactions, even in absence of catalyst (Fig. 8a and b). These developed vitrimers exhibit self-healing behavior at 180 °C for 30 min (healing efficiency = 92.9%) and shape memory at 100 °C for both EMDA-AA and EMDA-AA-CF (Fig. 8c and d). The

RSC Advances Review

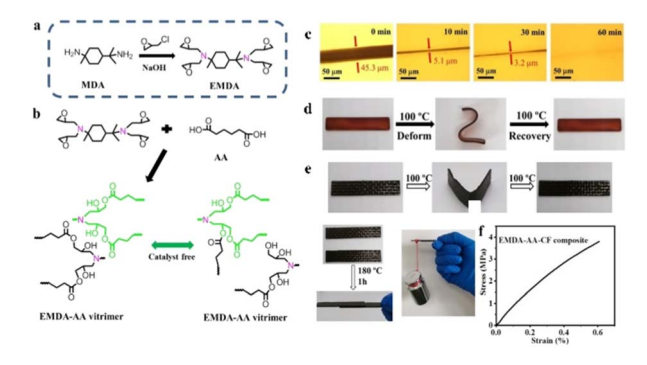


Fig. 8 Schematic diagrams of (a) the EMDA production method and (b) the EMDA-AA vitrimer curing reaction. (c) Healing behaviour at different heating times for EMDA-AA vitrimer. (d) Shape memory photographs of EMDA-AA. (e) Photographs of EMDA-AA-CF composites before and after self-adhering tests. The self-adhered composites are capable of lifting a weight of 500 g. The stress-strain curve of welded composites was determined using a lap-shear test.⁸⁴

reported epoxy vitrimer based composite shows good adhering properties (lap shear strength = 3.8 MPa), when two EMDA-AA-CF composites are bonded together under a hot press at 180 °C and 15 MPa (Fig. 8e).

Overall, catalyst promoted exchangeable transesterification reactions are more often reported, 102-105 whereas, participation of neighbouring groups as well as internal catalysis could be advantageous in terms of catalyst cost and environmental impact, 106,107 thus, requires more attention of researcher for developing sustainable vitrimers.

3.2 Disulfide exchange reactions

Since a long time, the active and fragile behaviour of disulfide bonds has been commonly used for the development of vulcanized rubber and proteins. Under specific conditions, disulfide bonds get reversibly broken, and swapped with bond dissociation energies around 210–270 kJ mol; therefore, disulfide bond exchange offers an enormous scope to develop recyclable and reformable thermosets while preserving their original strength. Note that disulphide exchange progresses in different manners, depending on ex. radical species or the presence of base. Readers should consider the proper exchange mechanism, considering the triggers for the exchange.

Recently, Weidmann and co-workers reported the thermoformability of carbon fiber reinforced vitrimer composites (vitrimer-CFRPC) base on epoxy formulations with disulfide crosslinkers, 113 where viscosity was investigated by means of a torsion clamp rheometer and tempered 3-point bending thermoforming. This study found that in contrast to thermoplastic-CFRPC no ply sliding was obtained in vitrimer-CFRPC, which could be due to the high matrix viscosity even at high temperatures above the $T_{\rm g}$ of the vitrimer-CFRPC. Opposite forming radii in a thermoformed omega profile lead to additional interlaminar shear forces, and thus these additional shear forces promote ply sliding and avoid the development of wrinkles and fiber damage. It could be demonstrated, that thermoforming of vitrimer-CFRPC based on sulfur bridges

is possible with only a few or little defects. In another report, Zhou and co-workers synthesized an aromatic amine curing agent containing dynamic disulfide bonds and carbon–nitrogen bonds, which is used to cure epoxy resin (E51) to obtain a degradable thermosetting material with good heat resistance and mechanical properties (Fig. 9a). See The reported CFRP vitrimer composites demonstrate a high tensile strength (732 MPa) and interlaminar shear strength (71 MPa) due to strong and stable –C–N– bonds and cross-linked structure. The degradation of resin in 2-mercaptoethanol (2-ME) and the remolding of resin powder under heating conditions is achievable by the dynamic bond exchange reaction of –S–S– bonds (Fig. 9b and c).

A catalyst-free disulfide exchange vitrimer was reported using 4-mercaptophenol derived (4-hydroxyphenyl) disulfide (BHPDS) and (4-glycidyloxyphenyl) disulfide (BGPDS).89 The resulting material demonstrates better weldability and reprocessability in comparison to the conventional epoxy, synthesized using methyl hexahydrophthalic anhydride (MHHPA) as a curing agent. Due to the disulfide exchanges, a faster stress relaxation time (3600 s at 80 °C to 440 s at 130 °C) and an activation energy E_a (53.3 kJ mol⁻¹) was observed. The material exhibits a prominent reprocessing and welding at 180 °C with 13 kPa measured at different times (20, 40, and 60 min). Owing to the presence of a disulfide bond in the resin and a sulfhydryl group in the 1-octanethiol solvent, the degradation of specimens was observed at 100 °C in 6 h. The recycled resin could be reused upon evaporation of 1-octanethiol and achieved 100% closed-loop recycling.

Later on, Si and co-workers⁹⁰ have reported a comparative study between dual disulfide vitrimer and single disulfide vitrimer. The dual disulfide vitrimer was prepared by reacting epoxy monomer (4-glycidyloxyphenyl disulfide) with an amine curing agent (4-aminophenyl disulfide) whereas in case of single disulfide vitrimer aromatic disulfide based curing agent (AFD) was mixed with DGEBA epoxy resin (Fig. 10a). The dual disulfide vitrimer demonstrates outstanding properties with the $T_{\rm g}$ of 147 °C, the storage modulus (E') of 1.72 GPa, and the tensile strength of 63.1 MPa (at r.t.) due to high contents of aromatic bonds (Fig. 10b and c). Despite that, this vitrimer shows fast stress relaxation rate with τ ranges from 1.95 s (220 °C) to 782 s (160 °C) (Fig. 10d), due to the dual operative

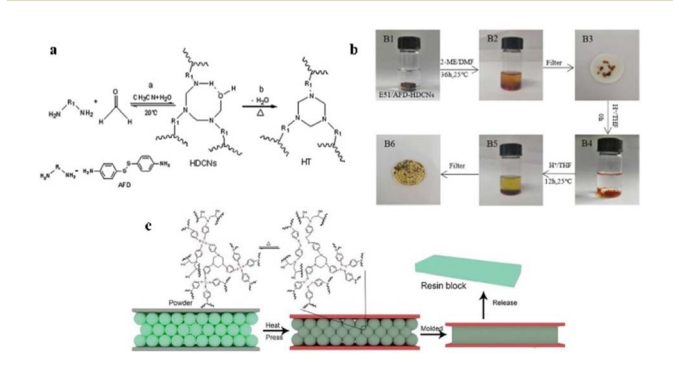


Fig. 9 (a) Diamine and formaldehyde reaction. (b) Degradation of AFD-HDCNs/E51 epoxy resin. (c) Schematic diagram of the reshaping process.⁸⁸

Review

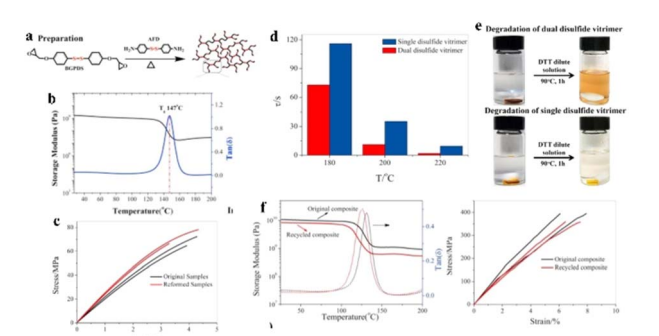


Fig. 10 (a) Synthesis of disulfide exchange based epoxy vitrimers. (b) Thermograms from dynamic mechanical analysis (DMA). (c) Tensile tests were used to compare the mechanical characteristics of the original and reformed samples. (d) At various temperatures, the relaxation periods of the dual disulfide vitrimer *versus* the single disulfide vitrimer. (e) At 90 °C, the solitary disulfide vitrimer partially degraded; the total concentration of DTT dilute solution was 0.1 mg ml⁻¹. (f) Original (black) and recycled (red) CFRP composites undergo DMA (left) and tensile testing (right).90

disulphide exchange, enabling the malleable and reprocessable abilities as well as the dissolution abilities in dithiothreitol (DTT) solution, at a miler condition compared with a single disulfide vitrimer (Fig. 10e). Moreover, the CFRP prepared by dual disulfide vitrimer exhibits excellent E' of 10.5 GPa and tensile strength of 334 MPa. After the degradation of epoxy vitrimer, the recycled carbon fibers were reformed again into CFRP with outstanding E' of 8.2 GPa and a tensile strength of 320.9 MPa (Fig. 10f), respectively.

It is highly essential to make a comparative study between the thermal and mechanical properties of diethyltoluenediamine (DETDA) (reference hardener) and 4-aminophenyl disulfide (AFD) (dynamic hardener) cured DGEBA. The dynamic epoxy-based network shows a rapid stress relaxation rate and τ ranges from 3 h at 130 °C to 20 s at 200 °C and activation energy ($E_{\rm a}$) of 55 kJ mol $^{-1}$ due to the reversible disulfide bridges in the dynamic network. The reshaping of the dynamic network takes place easily by hot pressing whereas the reference network breaks in the form of a powder. Furthermore, FRPCs were prepared by using dynamic network with new features of reprocessability, recyclability, and reparability. Even, the study found a comparable value of thermal and mechanical properties of the dynamic networks with the classical network obtained through diamine hardeners.

Overall, a catalyst free disulfide exchange has been a popular choice among dynamic exchange reactions. The dual disulfide exchange based vitrimeric materials seems very promising materials in terms of mechanical properties. However, the impact of fiber modification and interaction with matrix on bond exchange kinetics have not been a focus point and thus still needed more research.

3.3 Imine exchange reactions

Imine chemistry has been popular in materials science for a long time owing to its reversible bonding, which is currently considered an marvellous promise in dynamic covalent networks.75 Imine exchange promoted bio-based vitrimers are prepared from lignin-derived vanillin epoxy (VE) monomer and cured with four different types of curing agents such as 4,4'diaminodiphenylmethane (DDM), diethylenetriamine (DETA), isophoronediamine (IPDA), and polyetheramine D230. The $T_{\rm g}$ of VE-DDM, VE-IPDA, VE-IPDA-D230, and VE-DETA were reported as 143, 132, 84, and 58 °C, respectively. Owing to the rigidity of the amine-curing agent and cross-linking degree. Although, all samples are thermally stable up to 264 °C and their maximum decomposition temperature lies in the range of 314 to 370 °C. Moreover, the tensile strength at break (571 MPa) and Young's modulus (11.7 GPa) of CFRPs prepared through different epoxy systems was higher in the case of VE-IPDA due to better interfacial properties. All the epoxy systems are easily degradable in acidic solution. 93 In a similar study, two different imine exchange based vitrimers were synthesized using vanillin/1,6-hexylenediamine (VHP) and vanillin/m-xylylenediamine (VMP) curing agents. 4 The tan δ result shows that the T_{σ} of VHP and VMP bio-based imine epoxy vitrimers are 83 °C and 96 °C, respectively, whereas the storage modulus values are 2600 MPa and 2650 MPa, respectively. This could be attributed to the higher rigidity chain structure for VMP vitrimer (Fig. 12a and b). Furthermore, the CFRP prepared by VMP vitrimer exhibits an excellent tensile strength of 622 MPa which was close to those of CF/VHP of 584 MPa. The degradability of VMP and VHP vitrimers takes place under weakly acidic conditions, in which the imine bonds can be degraded into amino and aldehyde groups.

In addition, bio-based imine groups containing vitrimers were prepared by mixing vanillin/4-aminophenyl (VA) hardener with glycerol triglycidyl ether (Gte), in the presence of 1,2dimethylimidazole catalyst.59 The rigid network of Gte-VA due to the existence of π - π conjugate between the benzene ring and imine double bond resulted a high T_g (70 °C) and tensile strength (62 MPa). The Gte-VA vitrimer shows a fast relaxation rate (τ) of 3834 s at 120 °C and on further increasing the temperature to 130, 140, 150 and 160 °C it decreased to 2014, 1421, 814 and 431 s, respectively, while the activation energy (E_a) reaches 74.7 kJ mol-1. Bio-based imine system shows good reprocessability at 140 °C under 20 MPa pressure for 10 min. The reinforced Gte-VA vitrimer presents high tensile strength (449 MPa) and Young's modulus (12.9 GPa), as well as the recycled Gte-VA composite shows 574 MPa tensile strength and 13.7 GPa Young's modulus, respectively. Likewise, Memon and co-workers95 developed an imine curing hardener (ICH) based on vanillin and methylcyclohexanediamine (HDTA) and used it for the crosslinking of tri-functional epoxy resin (AFG-90H) (Fig. 11a). The prepared epoxy resin shows T_g of 131, 135, 138, and 136 °C, tensile strength of 82, 73, 58, and 63 MPa and the storage modulus of 2964, 3132, 3513, and 3801 MPa for pristine, 1st, 2nd, and 3rd reprocessed epoxy resin, respectively (Fig. 11b, c and d). Moreover, vitrimers exhibit fast stress relaxation upon heating and the associated activation energy (E_a) was 122 kJ mol⁻¹. CFRC-1 samples were fabricated with imine vitrimer under hot-press by using uncured carbon fiber prepregs and revealed the flexural strength and flexural modulus of 1028 MPa and 56 GPa (Fig. 11e), respectively, where the values

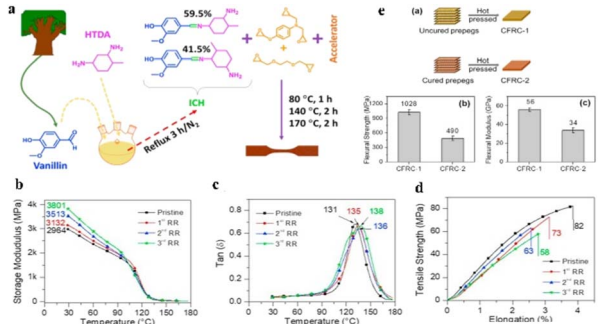


Fig. 11 (a) The ICH production and epoxy resin curing are depicted schematically. (b) Storage modulus, (c) $\tan \delta$, and (d) tensile strength–elongation curves of pristine and reprocessed epoxy resin.⁹⁵

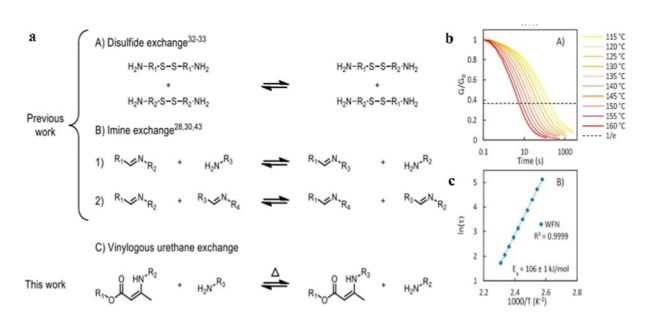


Fig. 12 (a) The two most often utilized dynamic exchange chemistries in amine-cured epoxy vitrimers, as well as the one employed in this study, are depicted in this diagram (A) disulfide exchange. (B) Imine exchange. (C) Vinylogous urethane exchange. (b) Stress relaxation experiment results. (c) The resulting relaxation periods are plotted using the Arrhenius method.⁹⁹

are relatively close to the conventional CFRP-epoxy resins. In contrast, CFRC-2 was fabricated using fully cured eight carbon fiber prepreg sheets. However, the results of flexural tests show that the flexural strength and modulus of CFRC-2 are only 490 MPa and 34 GPa, respectively, which are 47 and 60% of CFRC-1. The decrease in flexural performance of CFRC-2 might be due to the fact that the existence of carbon fibers prevents the epoxy resin from intimate contact and sufficient bond exchanges.

The development of a degradable matrix for FRPs leads to high costs and relatively low performance that limits their use in structural applications. Therefore, recently a new class of thermoset (polyaminal) was introduced based on imine/secondary amine dynamic bonds synthesized by imine aldehyde condensation, ⁹⁶ where terephthaldehyde and various diamines were used as monomers, and triethylenetetramine was selected as a novel cross-linker to prepare the degradable polyaminal. As triethylenetetramine contains -NH₂ and -NH-CH₂-CH₂-NH- groups, a hybrid imine/imidazolidine cross-linking structure was obtained. Due to rigid ring structure of imidazolidine, the polyaminal represents higher cross-linking density and mechanical properties compared with common thermosets based on Schiff base. The results showed that the

obtained degradable polyaminal exhibits superior properties, $T_{\rm g}$ (120–150 °C), $T_{\rm d}$ (249–277 °C), and tensile strength (52–64 MPa). In addition, the polyaminal/carbon fiber composites degrade completely under mild acidic conditions, leading a non-destructive recycling of fibers.

3.4 Other exchange reactions

Urethane exchange based vitrimeric materials were developed (TDNR) using toluene diisocyanate and novolac resin rich with phenolic hydroxyls,98 where diisocyanate phenolic-urethane vitrimer exhibits a covalent exchange based on reverse reaction chemistry due to excess aromatic hydroxyls and isocyanates. With glass transition temperature ranging from 80 °C to 230 °C, the reported vitrimer demonstrates good tensile strength (55 MPa), elongation at break (11-12%), and Young's modulus (1.1 GPa). The TDNR based glass fiber composites show the flexural strength and interlaminar shear strength values of 184.1 MPa and 12.93 MPa, respectively. Spiesschaert and co-workers99 have developed a vinylogous urethane (VU) bonds containing oligomeric amine curing agent. The polyfunctional amine-curing agent can be used as a drop-in solution for existing epoxy resin technologies, resulting in transparent, rigid and at the same time highly reprocessable catalyst-free epoxy vitrimer, demonstrates exchanges via transamination reaction (Fig. 12a). The oligomeric VU-curing agents were prepolymerized via a straightforward condensation reaction between acetoacetates extended with different classical amine monomers and epoxy hardeners. In addition, remarkably short processing time was observed in the absence of any catalyst, and the material displays very short stress relaxation time and good recyclability (Fig. 12b and c). Furthermore, a proof of concept for its use in obtaining glassfiber-reinforced epoxy composites is also reported, where the composites show excellent strength and elongation at failure values of 939 MPa and 2.5%, respectively. Denissen and coworkers have also explored a transamination exchange-based vitrimers using vinylogous urea network and amines and acetoamide monomers.100 The combination of these networks with a simple acid catalyst (0.5 mol% pTsOH) resulted good mechanical properties ($T_{\rm g} \sim 110$ °C, $E \sim 2.2$ GPa) and remarkably short relaxation times. Interestingly, vinylogous urea vitrimer based GFRP composites allow an efficient thermoforming as well as a thermal fusion of multilayers and recycling of fiber by solvolysis process.

4. The emerging applications of vitrimers based FRPs

Since fiber reinforced vitrimeric composites exhibit mechanical properties comparable to commercially utilized epoxy composites, vitrimeric materials have attracted the interest of industries involve in structural materials.³⁶ Along with good thermoforming reprocessability, repairability of delaminations and micro cracks by applying heat and pressure to the damaged part, and recyclability by matrix dissolving or grinding and reprocessing is highly advantageous.¹¹⁴ To

Review RSC Advances

manufacture woven carbon composites, malleable polyamine networks were utilised as a binder, demonstrating efficient closed-loop recycling of the fiber and binder ingredients. Due to the malleable nature of the polyamine binder network, cured CFRPs can be moulded into 3D curvature and multilayer devices can be built up using a simple heating process. 115 The incorporation of glass fibers improves the mechanical strength of shape memory epoxies that can be used in a variety of engineering applications. Self-folding origami structures, which were previously difficult to fold by hand, can now be easily designed using a topological change process regulated by dynamic ester bonds.116 Synthesizing a novel cyclolinear cyclotriphosphazane-based epoxy resin with a radial-mediated aromatic disulfide exchange mechanism, multifunctional and multi-responsive vitrimer systems have been produced, where high self-healing effectiveness of 89.8% proves to be promising candidate in aerospace and automotive industries. 117 The use of a bio-based vanillin-derived spiro diacetal structure in epoxy resin allows CFRPs and coatings to be stiff and degradable under mild acidic conditions. Furthermore, the spiro diacetal structures rapid cleavability allows for fiber recycling and easy removal of the coating from the substrate. 118 In addition, development of phosphonate-based intrinsic flame retardant vitrimer are claimed to overcome flame retardant additives in recyclable composite materials. Due to the enhanced residue yield and gas release, the vitrimer exhibits intumescent behaviour in fire. The phosphonate vitrimer-based glass and carbon fiber composites are particularly attractive in structural applications such as civil infrastructure and cars. 119 Fatigue failure in rotorcraft components begins with tiny size subcritical cracks that gradually evolve into macroscopic crack localization and eventually fail. By arresting incipient cracks, the DGEBA and adipic acid based epoxy vitrimer displays better fracture and fatigue performance. Therefore, the application of vitrimers in rotorcraft component induces self-healing along with better mechanical performance. 120 Through the use of an organic-inorganic matrix containing disulphide, the production of intrinsic low-temperature self-healing composites for medium-tech applications was proven. The GFRPs show multiple healing of flexural and interlaminar qualities as well as healing at minimum pressure for small scale (<cm²) damages.121 The fabrication of widely used polystyrene (PS) plastics based on the nitrogen coordinating cyclic boronic ester linkages served as a sensible roadmap for the development of dynamic materials through general-purpose plastics. The method offers a fresh approach to the creation of eco-friendly dielectric polymer materials for copper clad laminates. The PS vitrimer composites with glass fiber reinforcement exhibit good mechanical properties and can be easily recycled to obtain resin solution and clean glass fiber. 122 However, thermally and mechanically robust polymeric materials for copper clad laminates with low dielectric loss (D_r) are very scarce, therefore, a simple method to prepare cyclic polyolefin (COC)/ polystyrene vitrimers (PSVMs) from semi-interpenetrating polymer networks with low D_r were demonstrated and its quartz glass fiber composites exhibits excellent thermal,

mechanical, and dielectric properties for application in fifthgeneration mobile communications. ¹²³

5. Summary and outlook

In this review, we outlined the functional fiber-reinforced vitrimer with various bond exchange mechanisms. Through the present review paper, the special features of these materials, such as healability, reprocessability, and recyclability, were demonstrated, which are all thanks to the dynamic bond exchange. Furthermore, the categorised mechanisms are highlighted with their healing efficiency, and the proposed results are extremely useful in understanding the mechanical behaviour of vitrimeric materials. Especially, the demand for recyclable and healable composite materials with great mechanical strength must increase, considering the future development of high-class resins for automobile and aircraft industries. Moreover, these materials could be especially valuable in the aerospace industry and in high performance materials such as windblades, since replacement of the damaged resins cannot be made easily and thus self-healable resins are favourable. Numerous variables, such as the chemical structure of the polymer backbone, chain flexibility, the amount and nature of reactive sites responsible for healing, need to be considered before designing the futuristic materials. In addition to bond forming-breaking reactions other variables e.g., resin flow and their macroscopic deformation also need to be contemplated. Bio-based vitrimers are still limited but highly attractive, due to the increased demand to realize sustainable society. For true application of the fiber-reinforced vitrimers, the precise control of the bond exchange properties, including the activation temperature and the time scale of the bond exchange is very critical. A number of techniques are used to identify $T_{\rm v}$, those include stress relaxation, creep, and fluorescence. Among them stress relaxation is the most accurate technique due to its independence from procedural parameters such as heating rate, but non-isothermal creep testing is the quickest way to determine $T_{\rm v}$. Besides, researchers need a special attention while designing the polymer network based composites, e.g. quality of fillers, the strength of the filler/matrix interface, filler surface chemistry, filler geometry. In this regards, development of fundamental physics of vitrimer properties are required. Moreover, the rheological behaviour of the vitrimers in regard of manufacturing of fiber-reinforced composites need to be studied in more detail. The history of vitrimers are still a little over 10 years (since 2011), but these functional materials could find versatile application by collaboration of chemist and physicist, and academic/industrial researchers.

Conflicts of interest

There are no conflicts to declare.

Acknowledgements

We gratefully acknowledge the financial support from Science and Engineering Research Board (SERB-DST), Government of **RSC Advances** Review

India (Grant No. CRG/2021/006957). Part of this research work was performed within the COMET-Module project "Chemitecture" (project-no.: 21647048) and the COMET- K1 project "Polymers with reversibly adaptable surface properties by introducing multi-functional micropatterns" (project-no.: 1071910) at the Polymer Competence Center Leoben GmbH (PCCL, Austria) within the framework of the COMET-program of the Federal Ministry for Climate Action, Environment, Energy, Mobility, Innovation and Technology and the Federal Ministry for Digital and Economic Affairs with contributions by Montanuniversitaet Leoben (Department Polymer Engineering and Science). The PCCL is funded by the Austrian Government and the State Governments of Styria, Upper and Lower Austria. WHB acknowledges the International Graduate School (AGRIPOLY), funded by the State Saxony-Anhalt; as well as the DFG-funded CRC TRR 102/TP A03 for financial support.

References

- 1 D. K. Rajak, D. D. Pagar, R. Kumar and C. I. Pruncu, J. Mater. Res. Technol., 2019, 8, 6354-6374.
- 2 S. Vigneshwaran, R. Sundarakannan, K. M. John, R. D. Joel Johnson, K. A. Prasath, S. Ajith, V. Arumugaprabu and M. Uthayakumar, J. Cleaner Prod., 2020, 277, 124109.
- 3 H. Sharma, A. Kumar, S. Rana and L. Guadagno, Polymers, 2022, 14, 1548.
- 4 B. Wang, S. Ma, S. Yan and J. Zhu, Green Chem., 2019, 21, 5781-5796.
- 5 C. Zhang, J. Xue, X. Yang, Y. Ke, R. Ou, Y. Wang, S. A. Madbouly and Q. Wang, Prog. Polym. Sci., 2022, 125, 101473.
- 6 S. Utekar, V. K. Suriya, N. More and A. Rao, Composites, Part B, 2021, 207, 108596.
- 7 M. M. A. Nassar, K. I. Alzebdeh, T. Pervez, N. Al-Hinai and A. Munam, J. Appl. Polym. Sci., 2021, 138, 51284.
- 8 W. H. Binder, Self-healing polymers: from principles to applications, John Wiley & Sons, 2013.
- 9 F. Sordo and V. Michaud, Smart Mater. Struct., 2016, 25, 84012.
- 10 L. Guadagno, C. Naddeo, M. Raimondo, G. Barra, L. Vertuccio, A. Sorrentino, W. H. Binder and M. Kadlec, Composites, Part B, 2017, 128, 30-38.
- 11 W. H. Binder and R. Zirbs, in Advances in Polymer Science, ed. W. Binder, Springer Berlin Heidelberg, Berlin, Heidelberg, 2007, pp. 1-78.
- 12 S. Wang and M. W. Urban, Nat. Rev. Mater., 2020, 5, 562-583.
- 13 S. Chen and W. H. Binder, Acc. Chem. Res., 2016, 49, 1409-1420.
- 14 T. Yan, K. Schröter, F. Herbst, W. H. Binder and T. Thurn-Albrecht, Sci. Rep., 2016, 6, 32356.
- 15 A. G. Fallis, J. Chem. Inf. Model., 2013, 53, 1689-1699.
- 16 A. Voznyi, V. Kosyak, P. Onufrijevs, L. Grase, J. Vecstaudža, A. Opanasyuk and A. Medvid, J. Alloys Compd., 2016, 688,
- 17 R. Long, H. J. Qi and M. L. Dunn, Soft Matter, 2013, 9, 4083-4096.

- 18 Y. Zhang, H. Ying, K. R. Hart, Y. Wu, A. J. Hsu, A. M. Coppola, T. A. Kim, K. Yang, N. R. Sottos, S. R. White and J. Cheng, Adv. Mater., 2016, 28, 7646–7651.
- 19 L. Guadagno, L. Vertuccio, C. Naddeo, E. Calabrese, G. Barra, M. Raimondo, A. Sorrentino, W. H. Binder, P. Michael and S. Rana, Composites, Part B, 2019, 157, 1-13.
- 20 S. Rana, D. Döhler, A. S. Nia, M. Nasir, M. Beiner and W. H. Binder, Macromol. Rapid Commun., 2016, 37, 1715-1722.
- 21 M. Schunack, M. Gragert, D. Döhler, P. Michael and W. H. Binder, Macromol. Chem. Phys., 2012, 213, 205-214.
- 22 C. N. Bowman and C. J. Kloxin, Angew. Chem., Int. Ed., 2012, 51, 4272-4274.
- 23 A. Campanella, D. Döhler and W. H. Binder, Macromol. Rapid Commun., 2018, 39, 1700739.
- 24 L. Guadagno, L. Vertuccio, C. Naddeo, E. Calabrese, G. Barra, M. Raimondo, A. Sorrentino, W. H. Binder, P. Michael and S. Rana, *Polymers*, 2019, 11, 903.
- 25 V. K. Thakur and M. R. Kessler, *Polymers*, 2015, **69**, 369-383.
- 26 R. V. S. P. Sanka, B. Krishnakumar, Y. Leterrier, S. Pandey, S. Rana and V. Michaud, Front. Mater., 2019, 6, 137.
- 27 H. Fischer, Nat. Sci., 2010, 2, 873-901.
- 28 H. L. James Darnell and D. Baltimore, Gamete Res., 1987, 17,
- 29 D. Montarnal, M. Capelot, F. Tournilhac and L. Leibler, Science, 2011, 334, 965-968.
- 30 X. Chen, M. A. Dam, K. Ono, A. Mal, H. Shen, S. R. Nutt, K. Sheran and F. Wudl, Science, 2002, 295, 1698-1702.
- 31 H. Otsuka, Polym. J., 2013, 45, 879-891.
- 32 B. Krishnakumar, R. V. S. Prasanna Sanka, W. H. Binder, C. Park, J. Jung, V. Parthasarthy, S. Rana and G. J. Yun, Composites, Part B, 2020, 184, 107647.
- 33 W. Alabiso and S. Schlögl, *Polymers*, 2020, 12.
- 34 B. Krishnakumar, R. V. S. P. Sanka, W. H. Binder, V. Parthasarthy, S. Rana and N. Karak, Chem. Eng. J., 2020, 385, 123820.
- 35 M. Hayashi, Polymers, 2020, 12, 1322.
- 36 J. Zheng, Z. M. Png, S. H. Ng, G. X. Tham, E. Ye, S. S. Goh, X. J. Loh and Z. Li, Mater. Today, 2021, 51, 586-625.
- 37 M. L. Williams, R. F. Landel and J. D. Ferry, J. Am. Chem. Soc., 1955, 77, 3701-3707.
- 38 D. J. Lohse, S. T. Milner, L. J. Fetters, M. Xenidou, N. Hadjichristidis, R. A. Mendelson, C. A. García-Franco and M. K. Lyon, Macromolecules, 2002, 35, 3066-3075.
- 39 D. Montarnal, M. Capelot, F. Tournilhac and L. Leibler, Science, 2011, 334, 965-968.
- 40 H. Fang, H. Fang, H. Fang, W. Ye, Y. Ding, Y. Ding and H. H. Winter, Macromolecules, 2020, 53, 4855-4862.
- 41 Y. Nishimura, J. Chung, H. Muradyan and Z. Guan, J. Am. Chem. Soc., 2017, 139, 14881-14884.
- 42 M. Capelot, M. M. Unterlass, F. Tournilhac and L. Leibler, ACS Macro Lett., 2012, 1, 789-792.
- 43 X. Shi, Q. Ge, H. Lu and K. Yu, Soft Matter, 2021, 17, 2104-2119.
- 44 L. Li, X. Chen, K. Jin, M. Bin Rusayyis and J. M. Torkelson, Macromolecules, 2021, 54, 1452-1464.

Review

45 Y. Yang, S. Zhang, X. Zhang, L. Gao, Y. Wei and Y. Ji, *Nat. Commun.*, 2019, 1–8.

- 46 A. M. Hubbard, Y. Ren, P. Papaioannou, A. Sarvestani, C. R. Picu, D. Konkolewicz, A. K. Roy, V. Varshney and D. Nepal, ACS Appl. Polym. Mater., 2022, 4, 6374–6385.
- 47 S. Chen, T. Yan, M. Fischer, A. Mordvinkin, K. Saalwächter, T. Thurn-Albrecht and W. H. Binder, *Angew. Chem., Int. Ed.*, 2017, **56**, 13016–13020.
- 48 A. Ghosh and K. S. Schweizer, *ACS Macro Lett.*, 2021, **10**, 122–128.
- 49 K. Pahnke, J. Brandt, G. Gryn'ova, P. Lindner, R. Schweins, F. G. Schmidt, A. Lederer, M. L. Coote and C. Barner-Kowollik, *Chem. Sci.*, 2015, 6, 1061–1074.
- 50 N. K. Guimard, J. Ho, J. Brandt, C. Y. Lin, M. Namazian, J. O. Mueller, K. K. Oehlenschlaeger, S. Hilf, A. Lederer, F. G. Schmidt, M. L. Coote and C. Barner-Kowollik, *Chem. Sci.*, 2013, 4, 2752–2759.
- 51 K. Pahnke, J. Brandt, G. Gryn'ova, C. Y. Lin, O. Altintas, F. G. Schmidt, A. Lederer, M. L. Coote and C. Barner-Kowollik, Angew. Chem., Int. Ed., 2016, 55, 1514–1518.
- 52 J. Zhao, L. Debertrand, T. Narita and C. Creton, *J. Rheol.*, 2022, **66**, 1255.
- 53 A. Perego and F. Khabaz, J. Polym. Sci., 2021, 59, 2590-2602.
- 54 L. Qun-Li, X. Xiuyang, Y. Juan, P. C. Massimo and N. Ran, *Proc. Natl. Acad. Sci.*, 2020, **117**, 27111–27115.
- 55 A. Zandiatashbar, C. R. Picu and N. Koratkar, *Small*, 2012, 8, 1676–1682.
- 56 W. K. Goertzen and M. R. Kessler, *Mater. Sci. Eng. A*, 2006, 421, 217–225.
- 57 Y. Liu, Z. Tang, D. Wang, S. Wu and B. Guo, *J. Mater. Chem. A*, 2019, 7, 26867–26876.
- 58 S. Wang, S. Ma, Q. Li, X. Xu, B. Wang, K. Huang, Y. Liu and J. Zhu, *Macromolecules*, 2020, 53, 2919–2931.
- 59 Y. Y. Liu, G. L. Liu, Y. D. Li, Y. Weng and J. B. Zeng, ACS Sustainable Chem. Eng., 2021, 9, 4638–4647.
- 60 Y. Y. Liu, J. He, Y. D. Li, X. L. Zhao and J. B. Zeng, Compos. Commun., 2020, 22, 100445.
- 61 A. M. Hubbard, Y. Ren, A. Sarvestani, D. Konkolewicz, C. R. Picu, A. K. Roy, V. Varshney and D. Nepal, ACS Omega, 2022, 7, 29125–29134.
- 62 Z. Yang, Q. Wang and T. Wang, ACS Appl. Mater. Interfaces, 2016, 8, 21691–21699.
- 63 Y. Yang, Z. Pei, X. Zhang, L. Tao, Y. Wei and Y. Ji, *Chem. Sci.*, 2014, 5, 3486–3492.
- 64 G. kang Chen, K. Wu, Q. Zhang, Y. cen Shi and M. geng Lu, Macromol. Res., 2019, 27, 526–533.
- 65 Z. Huang, Y. Wang, J. Zhu, J. Yu and Z. Hu, *Compos. Sci. Technol.*, 2018, **154**, 18–27.
- 66 F. Hajiali, S. Tajbakhsh and M. Marić, *Polymer*, 2021, 212, 123126.
- 67 U. Shaukat, E. Rossegger and S. Schlögl, *Polymers*, 2021, 231, 29–34.
- 68 X. Chen, L. Li, T. Wei, D. C. Venerus and J. M. Torkelson, ACS Appl. Mater. Interfaces, 2019, 11, 2398–2407.
- 69 A. Legrand and C. Soulié-Ziakovic, *Macromolecules*, 2016, 49, 5893–5902.

- 70 Z. Huang, Y. Wang, J. Zhu, J. Yu and Z. Hu, Compos. Sci. Technol., 2018, 154, 18–27.
- 71 T. Kimura and M. Hayashi, Polym. J., 2022, 54, 1307-1319.
- 72 K. Tangthana-umrung and M. Gresil, Compos. Commun., 2022, 32, 101182.
- 73 I. Aranberri, M. Landa, E. Elorza, A. M. Salaberria and A. Rekondo, *Polym. Test.*, 2021, 93, 106931.
- 74 L. E. Porath and C. M. Evans, *Macromolecules*, 2021, 54, 4782–4791.
- 75 B. Krishnakumar, A. Pucci, P. P. Wadgaonkar, I. Kumar, W. H. Binder and S. Rana, *Chem. Eng. J.*, 2021, 133261.
- 76 K. Yu, Q. Shi, M. L. Dunn, T. Wang and H. J. Qi, *Adv. Funct. Mater.*, 2016, **26**, 6098–6106.
- 77 T. Farajpour, Y. Bayat, M. Abdollahi and M. H. Keshavarz, *J. Appl. Polym. Sci.*, 2015, **132**, 41936.
- 78 K. Yu, P. Taynton, W. Zhang, M. L. Dunn and H. J. Qi, *RSC Adv.*, 2014, 4, 48682–48690.
- 79 L. Yu, C. Zhu, X. H. Sun, J. Salter, H. A. Wu, Y. Jin, W. Zhang and R. Long, ACS Appl. Polym. Mater., 2019, 1, 2535–2542.
- 80 T. Liu, C. Hao, L. Shao, W. Kuang, L. Cosimbescu, K. L. Simmons and J. Zhang, *Macromol. Rapid Commun.*, 2021, 42, 2000458.
- 81 E. Chabert, J. Vial, J.-P. Cauchois, M. Mihaluta and F. Tournilhac, *Soft Matter*, 2016, **12**, 4838–4845.
- 82 M. Kamble, A. Vashisth, H. Yang, S. Pranompont, C. R. Picu, D. Wang and N. Koratkar, *Carbon*, 2022, **187**, 108–114.
- 83 T. Zhao, H. Bai, Z. Lei and R. Bai, *J. Phys.: Conf. Ser.*, 2012, 012034.
- 84 Y. Xu, S. Dai, L. Bi, J. Jiang, H. Zhang and Y. Chen, *Chem. Eng. J.*, 2022, **429**, 132518.
- Langenbach, C. Bakkali-Hassani, Q. Poutrel,
 Georgopoulou, F. Clemens, F. Tournilhac and
 Norvez, ACS Appl. Polym. Mater., 2022, 4, 1264–1275.
- 86 Q. Mu, L. An, Z. Hu and X. Kuang, *Polym. Degrad. Stab.*, 2022, **199**, 109895.
- 87 N. Lorwanishpaisarn, P. Kasemsiri, N. Srikhao, C. Son, S. Kim, S. Theerakulpisut and P. Chindaprasirt, *J. Appl. Polym. Sci.*, 2021, **138**, 1–12.
- 88 Q. Zhou, X. Zhu, W. Zhang, N. Song and L. Ni, *ACS Appl. Polym. Mater.*, 2020, **2**, 1865–1873.
- 89 H. Memon and Y. Wei, J. Appl. Polym. Sci., 2020, 137, 1-10.
- 90 H. Si, L. Zhou, Y. Wu, L. Song, M. Kang, X. Zhao and M. Chen, *Composites, Part B*, 2020, **199**, 108278.
- 91 A. Ruiz De Luzuriaga, R. Martin, N. Markaide, A. Rekondo, G. Cabañero, J. Rodríguez and I. Odriozola, *Mater. Horiz.*, 2016, 3, 241–247.
- 92 C. B. Cárdenas, V. Gayraud, M. E. Rodriguez, J. Costa, A. M. Salaberria, A. R. de Luzuriaga, N. Markaide, P. D. Keeryadath and D. C. Zapatería, *Polymers*, 2022, 14, 1222
- 93 Y. Wang, B. Jin, D. Ye and Z. Liu, Eur. Polym. J., 2022, 162, 110927.
- 94 X. Liu, E. Zhang, Z. Feng, J. Liu, B. Chen and L. Liang, *J. Mater. Sci.*, 2021, **56**, 15733–15751.
- 95 H. Memon, Y. Wei, L. Zhang, Q. Jiang and W. Liu, *Compos. Sci. Technol.*, 2020, **199**, 108314.

- 96 Y. Shen, N. Xu, Y. A. Adraro, B. Wang, Y. Liu, W. Yuan, X. Xu, Y. Huang and Z. Hu, ACS Sustainable Chem. Eng., 2020, 8, 1943–1953.
- 97 C. Ding, S. Zhang, M. Pan, M. C. Li, Y. Zhang and C. Mei, *Chem. Eng. J.*, 2021, 423, 130295.
- 98 X. Liu, Y. Li, X. Xing, G. Zhang and X. Jing, *Polymer*, 2021, 229, 124022.
- 99 Y. Spiesschaert, M. Guerre, I. De Baere, W. Van Paepegem, J. M. Winne and F. E. Du Prez, *Macromolecules*, 2020, 53, 2485–2495.
- 100 W. Denissen, I. De Baere, W. Van Paepegem, L. Leibler, J. Winne and F. E. Du Prez, *Macromolecules*, 2018, 51, 2054–2064.
- 101 X. An, Y. Ding, Y. Xu, J. Zhu, C. Wei and X. Pan, *React. Funct. Polym.*, 2022, **172**, 105189.
- 102 M. Hayashi and T. Inaba, ACS Appl. Polym. Mater., 2021, 3, 4424-4429.
- 103 M. Hayashi, ACS Appl. Polym. Mater., 2020, 2, 5365-5370.
- 104 F. Van Lijsebetten, J. O. Holloway, J. M. Winne and F. E. Du Prez, *Chem. Soc. Rev.*, 2020, 49, 8425–8438.
- 105 B. P. Krishnan, K. Saalwaechter, V. K. B. Adjedje and W. H. Binder, *Polymers*, 2022, 14.
- 106 S. Debnath, S. Kaushal and U. Ojha, ACS Appl. Polym. Mater., 2020, 2, 1006–1013.
- 107 D. Berne, F. Cuminet, S. Lemouzy, C. Joly-Duhamel, R. Poli, S. Caillol, E. Leclerc and V. Ladmiral, *Macromolecules*, 2022, 55, 1669–1679.
- 108 J. J. Griebel, R. S. Glass, K. Char and J. Pyun, *Prog. Polym. Sci.*, 2016, 58, 90–125.
- 109 H. Memon, Y. Wei and C. Zhu, *Polym. Test.*, 2022, **105**, 107420.

- 110 S. Nevejans, N. Ballard, J. I. Miranda, B. Reck and J. M. Asua, *Phys. Chem. Chem. Phys.*, 2016, **18**, 27577–27583.
- 111 C. J. Kloxin and C. N. Bowman, *Chem. Soc. Rev.*, 2013, 42(17), 7161-7173.
- 112 S. Sobczak, P. Ratajczyk and A. Katrusiak, *ACS Sustainable Chem. Eng.*, 2021, **9**, 7171–7178.
- 113 S. Weidmann, P. Volk, P. Mitschang and N. Markaide, *Composites, Part A*, 2021, **154**, 106791.
- 114 A. R. De Luzuriaga, A. Rekondo, R. Martín and N. Markaide, *FORMForum*, 2016, vol. 1–9.
- 115 P. Taynton, H. Ni, C. Zhu, K. Yu, S. Loob, Y. Jin, H. J. Qi and W. Zhang, Adv. Mater., 2016, 28, 2904–2909.
- 116 J. Zhu, G. Fang, Z. Cao, X. Meng and H. Ren, *Ind. Eng. Chem. Res.*, 2018, **57**, 5276–5281.
- 117 L. Zhou, G. Zhang, Y. Feng, H. Zhang, J. Li and X. Shi, *J. Mater. Sci.*, 2018, **53**, 7030–7047.
- 118 S. Ma, J. Wei, Z. Jia, T. Yu, W. Yuan, Q. Li, S. Wang, S. You, R. Liu and J. Zhu, *J. Mater. Chem. A*, 2019, 7, 1233–1243.
- 119 J. C. Markwart, A. Battig, T. Urbaniak, K. Haag, K. Koschek, B. Schartel and F. R. Wurm, *Polym. Chem.*, 2020, **11**, 4933–4941.
- 120 M. Kamble, C. Picu and N. Koratkar, 77th Annu. Vert. Flight Soc. Forum Technol. Display, FORUM 2021, Futur. Vert. Flight, 2021, pp. 1–5.
- 121 W. Post, A. Cohades, V. Michaud, S. van der Zwaag and S. J. Garcia, *Compos. Sci. Technol.*, 2017, **152**, 85–93.
- 122 S. Wang, B. Wang, X. Zhang, L. Wang, W. Fan, H. Li, C. Bian and X. Jing, *Appl. Surf. Sci.*, 2021, **570**, 151157.
- 123 S. Wang, L. Wang, B. Wang, H. Su, W. Fan and X. Jing, *Polymers*, 2021, 233, 124214.